IQ Imbalance Estimation Scheme with Intercarrier Interference Self-Cancellation Pilot Symbols in OFDM Direct Conversion Receivers

Hiroyuki Miyashita*, Mamiko Inamori*, Yukitoshi Sanada*, Teruji Ide†
*Department of Electronics and Electrical Engineering, Keio University, Yokohama, 223-8522 Japan
Email: miyashita@snd.elec.keio.ac.jp, {inamori,sanada}@elec.keio.ac.jp
†Department of Electronics and Electrical Engineering, Kagoshima National College of Technology, Kirishima, 899-5193 Japan
Email: t-ide@kagoshima-ct.ac.jp

***Abstract*—Direct conversion receivers in orthogonal frequency division multiplexing (OFDM) systems suffer from direct current (DC) offset, frequency offset, and IQ imbalance. We have proposed an IQ imbalance estimation scheme in the presence of DC offset and frequency offset, which uses pilot subcarriers in the frequency domain. In this scheme, the DC offset is eliminated by a differential filter. However, the accuracy of IQ imbalance estimation is deteriorated due to the intercarrier interference (ICI) components caused by frequency offset. To overcome this problem, a new IQ imbalance estimation scheme with intercarrier interference self-cancellation pilot symbols in the frequency domain has been proposed in this paper. Numerical results obtained through computer simulation show that estimation accuracy and bit error rate (BER) performance are improved.**

I. Introduction

Orthogonal frequency division multiplexing (OFDM) is one of modulation schemes for wireless communication to achieve high data transmission. The OFDM is standardized for WiMax, IEEE 802.11a/g, digital terrestrial broadcasting, and so on. At the receiving end, a direct conversion architecture has been implemented, which reduces the cost and power consumption of the receiver. However, OFDM direct conversion receivers may suffer from direct current (DC) offset, frequency offset, and IQ imbalance [1], [2]. The frequency offset is due to the mismatch between the oscillators in the transmitter and the receiver. The frequency offset at the receiver may deteriorate the orthogonality between the subcarriers and cause intercarrier interference (ICI). The DC offset is caused by the local oscillator (LO) signal. The LO signal may mix with itself down to zero intermediate frequency (IF), resulting in the generation of the DC offset. This is known as self-mixing and is due to the finite isolation that is typical between the LO and radio frequency (RF) ports of a low-noise amplifier (LNA) or mixers. Moreover, the DC offset is also attributed to the mismatch between the mixer components [1], [2]. The IQ imbalance arises mainly from the mismatches of the components between the in-phase (I) and quadrature (Q) paths. Specifically, phase mismatch occurs when the phase difference between the LO signals for the I and Q channels is not exactly 90 degrees [3]. These distortions deteriorate the quality of the demodulated signal.

Several joint compensation schemes have been presented [4]-[7]. However, these schemes assume the absence of the DC offset. On the other hand, in our previous research, the IQ imbalance is estimated in the presence of the DC offset and frequency offset [8], [9]. From the output of the differential filter, the IQ imbalance is estimated from a simple equation in the time domain. However, the accuracy of IQ imbalance estimation is deteriorated due to the intercarrier interference (ICI) components caused by frequency offset. Therefore, a new IQ imbalance estimation scheme with intercarrier interference self-cancellation pilot symbols in the frequency domain has been proposed in this paper. The proposed scheme uses a pair of pilot subcarriers to eliminate the influence of ICI. It works well if the frequency offset is relatively small.

II. IQ Imbalance Model with Frequency Offset

Assuming that the k^{th} sample of the OFDM preamble in the time domain is $s(k)$, a received signal only with the frequency offset, $r(k)$, is expressed as

$$r(k) = s(k)\exp(j\frac{2\pi\alpha}{N}k) + \omega(k), \tag{1}$$

where α is the frequency offset normalized by subcarrier separation, N is the number of samples for DFT, and $\omega(k)$ is the k^{th} additive white gaussian noise (AWGN) sample with zero mean and variance ${\sigma_n}^2$. In this paper, due to the symmetry of the upper and lower paths, the I-phase local signal, L_I, and the Q-phase local signal, L_Q, are assumed to be as follows:

I component $\quad L_I(t) = (1+\beta)\cos(2\pi f_c t - \theta/2)$,
Q component $L_Q(t) = -(1-\beta)\sin(2\pi f_c t + \theta/2)$,

where f_c is the carrier frequency, and the phase mismatch and the gain mismatch are represented as θ and β, respectively. These local signals are multiplied by the received signal. By applying a low pass filter (LPF), the baseband signals, $\hat{r}_I(k)$ and $\hat{r}_Q(k)$, with IQ imbalance are obtained. The k^{th} digitized signal with a sampling interval of T_s is given by

$$\hat{r}(k) \quad = \quad \hat{r}_I(k) + j\hat{r}_Q(k), \tag{2}$$

978-1-4673-0990-5/12/$31.00 ©2012 IEEE

where

$$\hat{r}_I(k) = (1+\beta)\{r_I(k)\cos(\frac{\theta}{2}) - r_Q(k)\sin(\frac{\theta}{2})\}, \quad (3)$$

$$\hat{r}_Q(k) = (1-\beta)\{r_Q(k)\cos(\frac{\theta}{2}) - r_I(k)\sin(\frac{\theta}{2})\}, \quad (4)$$

where $r_I(k)$ and $r_Q(k)$ are the I component and the Q component of $r(k)$, respectively. Hence, the complex baseband signal $\hat{r}(k)$ is

$$\begin{aligned}\hat{r}(k) &= \hat{r}_I(k) + j\hat{r}_Q(k) \\ &= \{\cos(\frac{\theta}{2}) + j\beta\sin(\frac{\theta}{2})\}\{r_I(k) + jr_Q(k)\} \\ &\quad + \{\beta\cos(\frac{\theta}{2}) - j\sin(\frac{\theta}{2})\}\{r_I(k) - jr_Q(k)\} \\ &= \{\cos(\frac{\theta}{2}) + j\beta\sin(\frac{\theta}{2})\}r(k) \\ &\quad + \{\beta\cos(\frac{\theta}{2}) - j\sin(\frac{\theta}{2})\}r^*(k) \quad (5)\end{aligned}$$

where * denotes complex conjugate. From Eq. (5), the received signal with the IQ imbalance is given as

$$\hat{r}(k) = \phi r(k) + \psi^* r^*(k) + \delta(k), \quad (6)$$

where

$$\phi = \cos(\frac{\theta}{2}) + j\beta\sin(\frac{\theta}{2}), \quad (7)$$

$$\psi = \beta\cos(\frac{\theta}{2}) + j\sin(\frac{\theta}{2}), \quad (8)$$

and $\delta(k)$ is the DC offset that occurs at the mixer.

III. Frequency Offset Estimation Using Differential Filter

In this frequency offset estimation scheme, the received signal with IQ imbalance is substituted into the differential filter used to eliminate the residual DC offset that passes through the HPF. The k^{th} output, $\hat{d}_{SP}(k)$, after the differential filter is

$$\begin{aligned}&\hat{d}_{SP}(k) \\ =\ &\hat{r}_{SP}(k) - \hat{r}_{SP}(k-1) \\ =\ &\phi\{r_{SP}(k) - r_{SP}(k-1)\} + \psi^*\{r^*_{SP}(k) - r^*_{SP}(k-1)\} \\ &+ \Delta\delta(k, k-1),\ k \geq 1, \quad (9)\end{aligned}$$

where

$$\hat{r}_{SP}(k) = \phi r_{SP}(k) + \psi^* r^*_{SP}(k), \quad (10)$$

$r_{SP}(k)$ is the k^{th} signal with the frequency offset in the STSP period, and $\Delta\delta(k, k-1)$ is the difference between the k^{th} and $(k-1)^{\text{th}}$ residual DC offsets. In IEEE 802.11a/g standards, the coarse frequency offset estimation is carried out in STSP and the fine frequency offset estimation is carried out in LTSP [10], [11]. In this paper, the estimated value of frequency offset, $\hat{\alpha}$, is calculated from auto-correlation value of STSP and LTSP received signals with IQ imbalance and frequency offset [9].

IV. IQ Imbalance Estimation

A. Conventional Scheme

1) IQ Imbalance Estimation in the absence of Frequency Offset: In the proposed scheme, the pilot subcarriers in the data period are used for IQ imbalance estimation. If the frequency offset does not exist, the l^{th} received symbol in the frequency domain after DFT, $\hat{R}(l)$, is given as

$$\hat{R}(l) = \phi(l)R(l) + \psi^*(-l)R^*(-l), \quad (11)$$

with

$$R(l) = \begin{cases} S(l) & l \in \mathbf{N_D}, \\ P(l) & l \in \mathbf{N_P}, \end{cases} \quad (12)$$

where $S(l)$ is the l^{th} data subcarrier, $P(l)$ is the l^{th} pilot subcarrier, $\mathbf{N_D}$ is the set of indices for the data subcarriers, and $\mathbf{N_P}$ is the set of indices for the pilot subcarriers. In Eq. (11), $\phi(l) = \phi H(l)$, $\psi(l) = \psi H(l)$, and $H(l)$ is the channel response of the l^{th} subcarrier. From Eq. (11), the symbol on the l^{th} subcarrier OFDM symbol is affected by the the symbol on the $(-l)^{\text{th}}$ subcarrier due to the IQ imbalance. To estimate the IQ imbalance, the pilot symbols shown in Table I are transmitted. The IQ imbalance is estimated from the m^{th} and $(m+1)^{\text{th}}$ consecutive OFDM symbols. Those two pilot symbols are written as

$$\hat{P}_m(l) = \phi(l)P_m(l) + \psi^*(-l)P^*_m(-l), \quad (13)$$

$$\hat{P}_{m+1}(l) = \phi(l)P_{m+1}(l) + \psi^*(-l)P^*_{m+1}(-l). \quad (14)$$

The mirror subcarriers of Eqs. (13) and (14) are also written as

$$\hat{P}_m(-l) = \phi(-l)P_m(-l) + \psi^*(l)P^*_m(l), \quad (15)$$

$$\hat{P}_{m+1}(-l) = \phi(-l)P_{m+1}(-l) + \psi^*(l)P^*_{m+1}(l). \quad (16)$$

By substituting the values of the pilot symbols from Table I into Eqs. (13)-(16), ϕ and ψ are calculated as

$$\psi^*(-l) = \frac{\hat{P}_m(l) + \hat{P}_{m+1}(l)}{2}, \quad (17)$$

$$\phi(l) = \frac{\hat{P}_m(l) - \hat{P}_{m+1}(l)}{2}, \quad (18)$$

$$\phi(-l) = \frac{\hat{P}_m(-l) + \hat{P}_{m+1}(-l)}{2}, \quad (19)$$

$$\psi^*(l) = \frac{\hat{P}_m(-l) - \hat{P}_{m+1}(-l)}{2}. \quad (20)$$

From Eqs. (17) to (20), it is given as

$$\frac{\psi^*}{\phi^*} = \frac{\psi^*(-l) + \psi^*(l)}{\phi^*(l) + \phi^*(-l)}, \quad \text{for } l \in \mathbf{N_P}. \quad (21)$$

Thus, the following equation is derived.

$$\frac{\psi^*}{\phi^*} = \varepsilon. \quad (22)$$

TABLE I
PILOT SUBCARRIERS OF CONVENTIONAL SCHEME.

Subcarrier number	-21	-7	7	21
m^{th} symbol	1	1	1	1
$(m+1)^{\text{th}}$ symbol	1	1	-1	-1

TABLE II
PILOT SUBCARRIERS OF PROPOSED SCHEME.

Subcarrier number	-22	-21	-8	-7	7	8	21	22
$2m^{\text{th}}$ symbol	-1	1	-1	1	1	-1	1	-1
$(2m+1)^{\text{th}}$ symbol	-1	1	-1	1	-1	1	-1	1

Here, with the assumption of small θ, ϕ and ψ are approximated as

$$\phi = \cos(\frac{\theta}{2}) + j\beta\sin(\frac{\theta}{2}) \approx 1 + j\beta\frac{\theta}{2}, \quad (23)$$

$$\psi = \beta\cos(\frac{\theta}{2}) + j\sin(\frac{\theta}{2}) \approx \beta + j\frac{\theta}{2}, \quad (24)$$

using the first-order approximation of the Taylor expansion. Thus, Eq. (22) becomes

$$\frac{\beta - j\frac{\theta}{2}}{1 - j\beta\frac{\theta}{2}} \approx \varepsilon_I + j\varepsilon_Q. \quad (25)$$

The estimated $\hat{\beta}$ and $\hat{\theta}$ can then be calculated as follows.

$$\hat{\beta} \approx \frac{2\varepsilon_I}{2 - \varepsilon_Q\hat{\theta}}, \quad (26)$$

$$\hat{\theta} \approx \frac{-(\varepsilon_I^2 + \varepsilon_Q^2 - 1) - \sqrt{(\varepsilon_I^2 + \varepsilon_Q^2 - 1)^2 + 4\varepsilon_Q^2}}{\varepsilon_Q}. \quad (27)$$

In the data period, the received signal is compensated with the estimations of ϕ and ψ given in Eqs. (7) and (8). The received symbol after IQ imbalance compensation, $\tilde{R}(l)$, is expressed as

$$\tilde{R}(l) = \frac{\phi^*\hat{R}(l) - \psi^*\hat{R}(-l)}{|\phi|^2 - |\psi|^2}, \quad \text{for } l \in \mathbf{N_D} \cup \mathbf{N_P}. \quad (28)$$

If the IQ imbalance is compensated completely, Eq. (28) is given as

$$\tilde{R}(l) = H(l)R(l), \quad \text{for } \ l \in \mathbf{N_D} \cup \mathbf{N_P}. \quad (29)$$

The compensated symbol shown in Eq. (29) contains the channel response on the l^{th} subcarrier. From the estimated channel response on each pilot subcarrier, the channel response of the other subcarriers are compensated with the 1^{st} order interpolation.

2) IQ Imbalance Estimation in the presence of Frequency Offset: In the time domain, the frequency offset causes additional phase rotation in the data period. The frequency offset is estimated and compensated in the time domain and IQ imbalance estimation is carried out in the frequency domain as shown in Fig. 1. From Eq. (6), the k^{th} received signal after

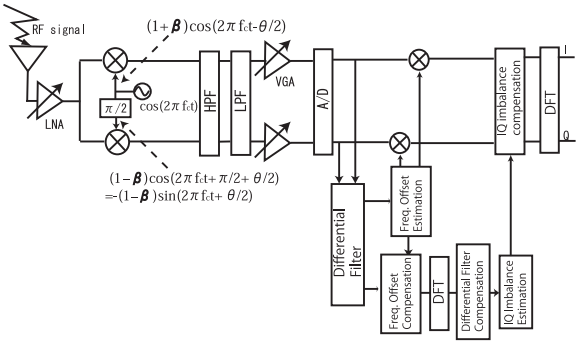

Fig. 1. Receiver architecture of conventional scheme.

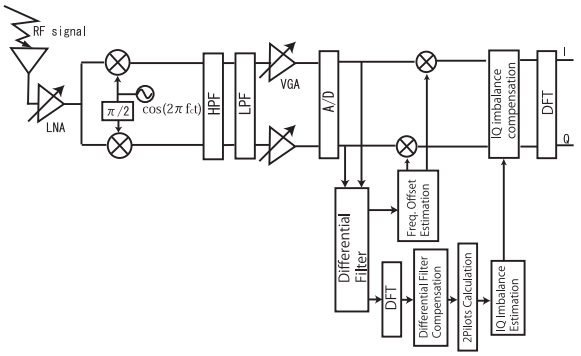

Fig. 2. Receiver architecture of proposed scheme.

frequency offset compensation in the time domain, $\hat{r}^{'}(k)$, is expressed as

$$\hat{r}^{'}(k) = \phi r(k) + \psi^* r^*(k)\exp(-j\frac{2\pi(\alpha+\hat{\alpha})}{N}k). \quad (30)$$

Here, the estimated frequency offset is given as $\hat{\alpha}$. The received symbol with the frequency offset in the frequency domain, $\hat{R}^{'}(l)$, is then given as

$$\begin{aligned} & \hat{R}^{'}(l) \\ = & \sum_{k=0}^{N-1}\hat{r}^{'}(k)\exp(-j\frac{2\pi l}{N}k) \\ = & \phi R(l) + \frac{\psi^*}{N}\Big(\sum_{k=0}^{N-1}R^*(-l)\exp(-j\frac{2\pi(\alpha+\hat{\alpha})}{N}k) \\ + & \sum_{k=0}^{N-1}\sum_{\substack{n=-\frac{N}{2} \\ n\neq -l}}^{\frac{N}{2}-1}R^*(n)\exp(-j\frac{2\pi(n+l)}{N}k)\exp(-j\frac{2\pi(\alpha+\hat{\alpha})}{N}k)\Big). \end{aligned} \quad (31)$$

From Eq. (31), it is shown that all the subcarriers cause ICI to the l^{th} subcarrier which deteriorates the accuracy of IQ imbalance estimation. Moreover, the averaging does not ignore the accuracy since the ICI components are affected by the frequency offset.

B. Proposed Scheme

The simulation model of proposed scheme is shown in Fig. 2. In this proposed scheme, the frequency offset estimation is not carried out, and then the IQ imbalance is estimated with a pair of pilot subcarriers in the frequency domain from the output of the differential filter.

From Eq. (6), the k^{th} output, $\hat{d}(k)$, after the differential filter is

$$\begin{aligned} & \hat{d}^{'}(k) \\ = \; & \hat{r}(k) - \hat{r}(k-1) \\ = \; & \phi(s(k)\exp(j\frac{2\pi\alpha}{N}k) - s(k-1)\exp(j\frac{2\pi\alpha}{N}(k-1))) \\ + \; & \psi^{*}(s^{*}(k)\exp(-j\frac{2\pi\alpha}{N}k) - s^{*}(k-1)\exp(-j\frac{2\pi\alpha}{N}(k-1))). \end{aligned} \tag{32}$$

Thus, the received symbol with the frequency offset after DFT in the frequency domain, $\hat{R}^{'}(l)$, is then given as

$$\hat{R}^{'}[l]$$

$$= \frac{\phi}{N}\Big\{\sum_{k=0}^{N-1} R[l]\exp(j\frac{2\pi\alpha}{N}k) \tag{33a}$$

$$+ \sum_{\substack{n=-\frac{N}{2} \\ n\neq l}}^{\frac{N}{2}-1} R[n]\frac{1-\exp(j2\pi(n+\alpha-l))}{1-\exp(j\frac{2\pi(n+\alpha-l)}{N})}\Big\} \tag{33b}$$

$$- \frac{\phi}{N}\Big\{\sum_{k=0}^{N-1} R[l]\exp(j\frac{2\pi\alpha}{N}k)\exp(-j\frac{2\pi(\alpha+l)}{N}k) \tag{33c}$$

$$+ \sum_{\substack{n=-\frac{N}{2} \\ n\neq l}}^{\frac{N}{2}-1} R[n]\frac{1-\exp(j2\pi(n+\alpha-l))}{1-\exp(j\frac{2\pi(n+\alpha-l)}{N})}\exp(-j\frac{2\pi(\alpha+n)}{N}k)\Big\} \tag{33d}$$

$$+ \frac{\psi^{*}}{N}\Big\{\sum_{k=0}^{N-1} R^{*}[-l]\exp(-j\frac{2\pi\alpha}{N}k) \tag{33e}$$

$$+ \sum_{\substack{n=-\frac{N}{2} \\ n\neq -l}}^{\frac{N}{2}-1} R^{*}[n]\frac{1-\exp(-j2\pi(n+\alpha-l))}{1-\exp(-j\frac{2\pi(n+\alpha-l)}{N})}\Big\} \tag{33f}$$

$$- \frac{\psi^{*}}{N}\Big\{\sum_{k=0}^{N-1} R^{*}[-l]\exp(-j\frac{2\pi\alpha}{N}k)\exp(-j\frac{2\pi(\alpha-l)}{N}k) \tag{33g}$$

$$+ \sum_{\substack{n=-\frac{N}{2} \\ n\neq -l}}^{\frac{N}{2}-1} R^{*}[n]\frac{1-\exp(-j2\pi(n+\alpha-l))}{1-\exp(-j\frac{2\pi(n+\alpha-l)}{N})}\exp(j\frac{2\pi(\alpha+n)}{N}k)\Big\}. \tag{33h}$$

From Eq. (33), it is shown that all the subcarriers cause ICI to the l^{th} subcarrier. Fig. 3 displays the vector representation of the interference on the 7^{th} subcarrier as shown in Eq. (33b) and Fig. 4 also displays the vector representation of the interference on the 8^{th} subcarrier as shown in Eq. (33b) ($R[l] = -1$, for $l \in \mathbf{N_D}$). From those figures, it is clear

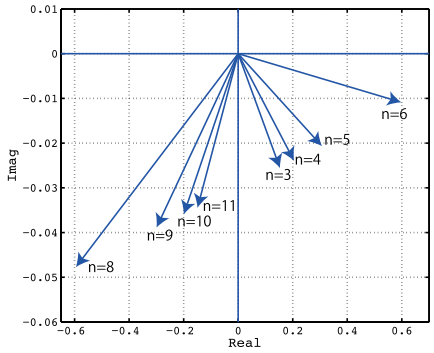

Fig. 3. Interference components Eq.(33b) on pilot subcarrier number 7 ($\alpha = 0.01$)

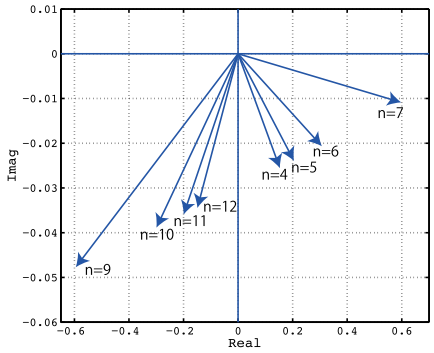

Fig. 4. Interference components Eq.(33b) on pilot subcarrier number 8 ($\alpha = 0.01$)

that the vectors of adjacent subcarriers on n^{th} subcarrier point toward almost the same direction. Therefore, if $(l\pm1)^{\text{th}}$ output, $\hat{R}'[l \pm 1]$, is subtracted from n^{th} subcarrier, the influence of ICI can be reduced. The IQ imbalance estimation is carried out with a pair of pilot symbols.

The subtracted output between adjacent subcarriers in the proposed IQ imbalance estimation scheme, $P'_m[l]$, is written as

$$\hat{P}_m[l] = \begin{cases} \hat{R}'_m[l] - \hat{R}'_m[l+1], & \text{for l=7,21} \\ \hat{R}'_m[l] - \hat{R}'_m[l-1]. & \text{for l=-7,-21} \end{cases} \tag{34}$$

The IQ imbalance is estimated with the same equations as conventional scheme and ϕ and ψ are calculated from Eq. (17) to Eq. (20).

V. Simulation Results

A. Simulation Conditions

The MSE of the IQ imbalance estimation and BER calculation is evaluated through computer simulation. Number of trials is 10,000 times. Information bits are modulated with QPSK in the preamble period and 64QAM in the data period on each subcarrier. The number of DFT/IDFT points is set to 64 while 52 subcarriers are used for the LTSP symbols,

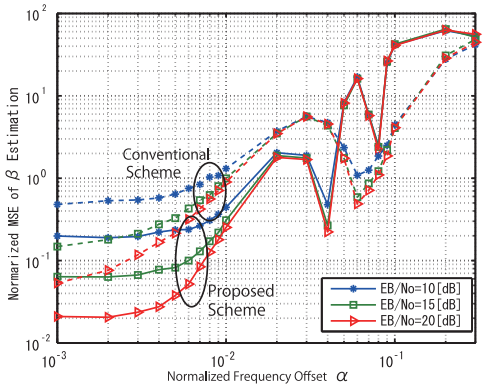

Fig. 5. Normalized MSE performance of gain mismatch estimation (β=0.05, θ=5[degree]).

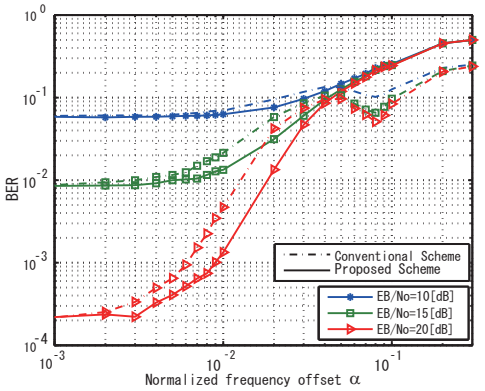

Fig. 6. BER vs. normalized frequency offset α (64QAM, β=0.05, θ=5[degree]).

which follows the IEEE 802.11a/g standard. The 1st order butterworth filter is employed as the Rx HPF. The cutoff frequency of the received HPF is set to 10[kHz]. The DC offset is set to 10[dB] [12]. The normalized frequency offset is from 0.001 to 0.3. The mismatch of amplitude is set to 0.05 and the mismatch of phase is set to 5[degree] [7].

B. Normalized MSE Performance vs. Frequency Offset

Figure 5 shows the normalized MSE performance of gain mismatch estimation, when the frequency offset α is varied. The gain mismatch β is set to 0.05 and the phase mismatch θ is set to 5[degree]. E_b/N_0 is set to {10, 15, or 20}[dB]. In this figure, 'Conventional scheme' refers to the IQ imbalance estimation scheme in the time domain as shown in [9]. It is clear that the proposed scheme is superior to the convectional scheme when the frequency offset α is less than 0.04. However, the MSE performance of the proposed scheme is deteriorated as the frequency offset increases. This is because the vectors as shown in Fig. 3 do not converge when the frequency offset becomes large, and influence of ICI remains even after subtraction between adjacent subcarriers.

C. BER Performance vs. Frequency Offset

Figure 6 shows the BER performance versus the normalized frequency offset α. The gain mismatch β is set to 0.05, the phase mismatch θ is set to 5[degree], and the frequency offset α ranges from 0.001 to 0.3. The BER performance of the proposed scheme is superior to the conventional scheme when the normalized frequency offset α is less than 0.04.

VI. Conclusion

In this paper, a low-complexity IQ imbalance estimation scheme in the presence of the DC offset and the frequency offset has been proposed. The conventional scheme uses the preamble signals in the time domain. However, the BER performance is deteriorated when the frequency offset is small. In the proposed IQ imbalance estimation scheme, a pair of pilot subcarriers in the frequency domain are employed. The numerical results obtained through computer simulation show that the proposed scheme works well and the BER performance of the proposed scheme is superior to the conventional scheme when the frequency offset is small.

Acknowledgments

This work is supported in part by a Grant-in-Aid for the Global Center of Excellence for high-Level Global Cooperation for Leading-Edge Platform on Access Spaces from the Ministry of Education, Culture, Sport, Science, and Technology in Japan.

References

[1] W. Namgoong and T. H. Meng, "Direct-Conversion RF Receiver Design," IEEE Trans. on Commun., vol.49, no.3, pp.518-529, Mar. 2001.

[2] R. Svitek and S. Raman, "DC Offsets in Direct-Conversion Receivers: Characterization and Implications," IEEE Microwave Magazine, vol.6, Issue 3, pp.76-86, Sept. 2005.

[3] T. Yuba and Y. Sanada, "Decision Directed Scheme for IQ Imbalance Compensation on OFCDM Direct Conversion Receiver," IEICE Trans. on Commun., vol.E89-E, no.1, pp.184-190, Jan. 2006.

[4] G. Xing, M. Shen, and H. Liu, "Frequency Offset and I/Q Imbalance Compensation for Direct Conversion Receivers," IEEE Trans. on Commun., vol.4, pp.673-680, Mar. 2005.

[5] G. T. Gil, I. H. Sohn, Y. H. Lee, Y. I. Song, and J. K. Park, "Joint ML Estimation of Carrier Frequency, Channel, I/Q Mismatch, and DC Offset in Communications Receivers," in IEEE Trans. on Veh. Tech., vol.54, no.1, pp.338-349, Jan. 2005.

[6] S. D. Rore, E. L. Estraviz, F. Horlin, and L. V. Perre, "Joint Estimation of Carrier Frequency Offset and IQ Imbalance for 4G Mobile Wireless Systems," Proc. of ICC'06, vol.5, pp.2066-2071, June 2006.

[7] J. Tubbax, A. Fort, L. V. Perre, S. Donnay, M. Moonen, and H. D. Man, "Joint Compensation of IQ Imbalance and Frequency Offset in OFDM Systems," Proc. of GLOBECOM'03, vol.3, pp.2365-2369, May 2003.

[8] M. Inamori, A. B. Bostamam, Y. Sanada, and H. Minami, "IQ Imbalance Compensation Scheme in the Presence of Frequency Offset and Dynamic DC Offset for a Direct Conversion Receiver," IEEE Trans. on Wireless Commun., vol.8, no.5, pp.2214-2220 (Correspondence), May 2009.

[9] M. Inamori, S. Takayama, and Y. Sanada, "IQ Imbalance Estimation Scheme in the Presence of DC Offset and Frequency Offset in the Frequency Domain," IEICE Trans. on Fundamentals, vol.E92-A, no.11, pp.2688-2696, Nov. 2009.

[10] IEEE.802.11a-Part 11, Wireless LAN Medium Access Control (MAC) and Physical Layer (PHY) Specifications; Highspeed Physical Layer in the 5GHz Band.

[11] IEEE.802.11g-Part 11, Wireless LAN Medium Access Control (MAC) and Physical Layer (PHY) Specifications; Highspeed Physical Layer in the 2.4GHz Band.

[12] M. Inamori, A. M. Bostamam, Y. Sanada, and H. Minami, "Frequency Offset Estimation Scheme in the Presence of Time-varying DC Offset for OFDM Direct Conversion Receivers," IEICE Trans. on Commun., vol.E90-B, no.10, pp.2884-2890, Oct. 2007.